Proceedings of the Institute of Acoustics

IDENTIFICATION OF THE CAUSE OF FAILURE OF AIRCRAFT STRUCTURES FROM COCKPIT VOICE RECORDERS

S J C Dyne and J K Hammond

Institute of Sound and Vibration Research, University of Southampton

Abstract

This paper discusses the identification of the cause of failure of aircraft structures due to explosive detonation or rapid decompression by examination of transducer recordings up to the time of failure. The use of cockpit voice recorders as a hybrid measurement of cabin pressure and microphone mounting vibration is discussed. The paper describes the mathematical models which have been used to predict the blast wave and decompression effects and these are compared with results from trials involving detonation of explosives and decompression on a static aircraft hull.

Introduction

Identification of the cause of failure is of fundamental importance following the loss of an aircraft. The flight data recorder and cockpit voice recorder can usually be recovered with the recordings intact after such a loss; even when an accident occurs over water, when recovery of the aircraft structure is often not possible. The flight data recorder is used to record the state of the aircraft and ancillary equipment at periodic intervals at low data rates (maximum 64 times/second) and so is inappropriate for the measurement of violent events which are high frequency phenomena. However, the cockpit voice recorder (CVR) is used to record voice communication on the flight deck and for audio identification of other cockpit sounds. It is therefore a high bandwidth device - current specifications [1] recommend a bandwidth of 5kHz - and is potentially useful for the identification of the violent event leading to the loss of the aircraft.

A series of experiments have shown that the CVR signatures of rapid decompression and explosive detonation are not as straightforward as negative or positive pressure pulses. There are several plausible explanations for this:

- The CVR microphone responds to vibration of its mounting in addition to pressure fluctuations.
- The microphone output is passed through an automatic gain control circuit which may cause a change in signal phase and amplitude before recording.

- The CVR system is not dc coupled so a step change in pressure will not produce a step change in the recording.

- Detonation of explosives produces a bipolar pressure fluctuation (i.e. both positive and negative gauge pressures).

- The pressure fields produced by both rapid decompression and explosive detonation are complex due to internal reflections and other wave phenomena acting on the pressure/shock waves.

A research programme has therefore been established to investigate the use of CVR recordings to identify the cause of failure and to explore the possibilities of using alternative transducers, e.g. accelerometers and pressure transducers [2,3,4].

Trials have been conducted on a variety of civil aircraft. In this paper we shall concentrate on the results of explosive detonation and rapid decompression tests on a Hawker Siddeley 125 aircraft - figure 1. Before the trials the engines, wings, tail control surface and cabin furniture were removed from the aircraft which was then mounted on a pair of wooden trestles. Small charges were detonated in the aircraft and recordings were made from pressure transducers and accelerometers in addition to the CVR cockpit area microphone (CAM) recordings. The same instrumentation was subsequently used for decompression tests: The aircraft was initially pressurised to 0.3 bar and decompression was achieved by removing a restraining plate from a diaphragm inserted in place of a passenger window. The pressure difference caused the diaphragm to rupture and led to decompression as the compressed gas expanded into the atmosphere. A selection of the ensuing CVR and instrumentation time histories are reproduced below. Figures 2 and 3 show the CVR time histories for blast and decompression respectively. The first few milliseconds are shown in expanded form in figures 4 and 5. Figures 6 and 7 show the corresponding acceleration time histories, and figure 8 and 9 again show an expanded time scale. Figures 10 and 11 show the signals recorded by a passenger cabin pressure transducer for blast and decompression respectively. Interpretation of these time histories has led to a study of mathematical models for the blast and decompression effects and these are considered in the next two sections of this paper.

Blast Wave Modelling

Following the detonation of an explosive, a spherical blast wave travels outwards at a velocity exceeding the speed of sound. Away from the immediate vicinity of the explosion an observer will see a sudden pressure rise when the blast wave arrives,

followed by a quasi-exponential decay to pressure below the initial ambient pressure and then a gradual restoration of ambient pressure. This ideal general form of pressure time history, which corresponds to the output of a pressure transducer in free spherical blast, is sketched in figure 12 and may be expressed as

$$p(t) = p_o(1-t/t_d)e^{-\alpha t/t_d}$$

In the expression p_o is the peak overpressure (at $t = 0$), t_d is the duration of the positive phase and α is a wave form parameter. A fourth parameter t_a gives the arrival time of the blast wave, this is the elapsed time between the detonation and the sudden increase in pressure at the measurement location. The term in parentheses provides the change in sign for the expression for $t > t_d$ and the last term in the expression gives the exponential form.

The magnitude of an explosion is customarily given in term of explosive yield [5] - this is defined as the mass of TNT which would release the same energy as the explosion. Note that TNT itself need not be involved in the explosion. TNT releases 4600kJ/kg, so a yield of say 100g will release 460kJ whatever explosive is used but this may require more or less than 100g of detonating material.

Scaling laws may be applied to a standard reference explosion to give approximate values to the parameters in the blast wave expression. Tables for a 1kg TNT explosion [5] have been used to construct the table below which records parameter values for explosions with yields of 2.5g and 250g at distances of 1m and 10m from the charge. The estimated yield of the detonator type charge used in trials described above is 2.5g; a charge of 250g would be likely to produce a non-elastic structural response.

The table shows that there is a wide variation in parameter values for the explosion measurements. The peak overpressure values cover a range of 50dB and so an instrument designed to measure all four explosions without *a priori* knowledge of the blast conditions would require a very wide dynamic range.

Table of blast wave parameter values

Yield(g)	Distance (m)	p_o (bar)	t_a (ms)	t_d (ms)	α
2.5	1	0.15	2.08	0.417	0.40
250	1	3.48	0.77	0.589	1.45
2.5	10	0.012	28.2	0.568	0.17
250	10	0.056	24.8	2.43	0.28

The arrival times should be compared with the time taken for sound to travel the same distance; at a velocity of $340ms^{-1}$ a sound wave takes 2.94ms to travel 1m and 29.4ms to cover 10m. The average blast wave speed is therefore greater than Mach 1 in every case, but is closer to the speed of sound at lower yield values and at larger distances.

The overpressure duration values give an indication of the minimum bandwidth required for an instrument to measure the blast wave. A sampling system would need to sample at a rate of 25kHz in order to capture at least 10 samples during the overpressure part of the waveform measured at 1m.

Signal Interpretation

Having now established a model for the blast wave, let us return to the experimental results which are reproduced below. How may we interpret these signals using the simple spherical model for the blast wave and the scaling laws? We begin with the blast wave pressure time history shown in figure 10. This curve shows a sudden pressure rise and positive pulse, but the gradual restoration of ambient pressure cannot be seen. This is because the blast wave is reflected from and diffracted by any objects in its path. The pressure transducer was mounted close to the ceiling of the aircraft cabin and multiple reflections of the blast wave produce a fluctuating pressure signal. However, the initial pulse stands out as a very clearly defined feature of the time history.

If we assume an uninterrupted path for the initial blast wave and we make use of the known location of the explosion and transducer, then the same scaling law which was used to construct the table above may also be used to estimate the yield of the explosive given the pressure time history. Note that after a real incident the approximate location of a charge may be known from charred wreckage and structural damage. For a peak overpressure of 0.155 bar and a distance of 0.9m the scaling law produces a yield estimate of 2.4g. This compares well with the estimated yield of 2.5g.

The accelerometer time history (figure 6) also displays some interesting features. Once again, before detonation the accelerometer records only background conditions. Following the blast, the time history displays two distinct regions; an almost harmonic constant amplitude section of amplitude 40g and duration 11ms is followed by a wide band section with a peak amplitude of 120g. To explain this observation let us consider what happens immediately following detonation. A blast wave travels outwards from the charge and rapidly reaches the walls of the aircraft. Wide band excitation of the wall close to the charge is then transmitted as structural vibration along the length of the aircraft to the accelerometer mounted in the cockpit and the transmission path filters the structural excitation to produce a harmonic response. The speed of this energy transmission through the structure is very high compared with the velocity of the blast

wave travelling through the air towards the cockpit. When this airborne blast wave reaches the panel on which the accelerometer has been mounted the local vibration becomes much larger in amplitude and covers a wider frequency range. The 11ms period can be compared with the arrival time for a blast wave travelling a distance of 4.6m: For a 2.5g charge, the scaling law gives an arrival time of 12.2ms.

The CVR signature shown in figures 2 and 4 is more difficult to interpret. It is believed that the CAM in the experimental configuration was able to respond effectively to vibration. Why then are the two distinct vibration modes shown in the accelerometer signal not seen? Furthermore, given that the CAM responds in some way to pressure excitation, why is the blast wave arrival not clearly visible? The answer probably lies in the automatic gain control (AGC) circuits of the CVR. The AGC is intended to change the sensitivity of the recording system according to background conditions: At high levels of background noise the AGC attenuates all incoming signals so that loud sounds may still be recorded without saturation of the CVR tape. At low levels of background noise the attenuation is reduced so that quiet sounds may still be recorded using the full dynamic range of the tape.

The initial structure borne vibration of 40g may be sufficient to cause AGC attenuation of the incoming signal. The arrival of the blast wave and peak vibrations of 120g simply cause further AGC attenuation so the blast wave arrival cannot be seen. The CVR signature is further complicated by the combination of both pressure and vibration into one signal. Other trials have shown a pre-cursor section in the CVR time histories similar to the accelerometer response before the local arrival of a blast wave. The characteristics of the pre-cursor will be related to; the magnitude of the excitation close to the charge and at the cockpit, the mechanical properties of the transmission path and CAM mounting and the AGC performance. This phenomenon, together with the possibility of reconstructing the signal prior to the automatic gain control from the CVR recording, is a topic of current interest.

We have now seen how the blast wave model leads to an understanding of the properties of the experimental data for explosive detonation. We consider next the effects of decompression and interpretation of the time histories following the rapid decompression of a pressurised hull.

Rapid Decompression

We shall consider two models for decompression. A simple thermo-fluid dynamics model for quasi-steady flow applied iteratively enables us to construct pressure curves for the pressure remaining in the aircraft cabin following the rapid removal of a

window, and a more refined non-steady flow model helps us to explain the detailed form of the results from trials. The means of achieving decompression in a static hull on the ground were discussed briefly in the introduction above.

The Quasi-steady Flow Model

If a tap were opened at the bottom of a barrel filled with water, the water would flow out at a rate depending on the depth of the water remaining. If this relation between flow rate and depth were known, it would be possible to calculate the volume of water leaving the barrel over a short interval δt. The calculated value for the volume could then be used to calculate the depth after δt to give a new flow rate. This iterative analysis of the problem could be used to predict the depth of water remaining at any time after the tap had been opened.

A similar iterative analysis may be applied to the aircraft when venting a compressed gas through a window which has been removed suddenly. In this case assumptions must be made about the compressed gas and about the expansion. For a simple model we assume the gas with pressure p, density ρ, and absolute temperature T is perfect, so that

$$\frac{p\rho}{T} = \text{constant}$$

Under steady adiabatic flow through a nozzle from a reservoir with upstream stagnation pressure p_o and density ρ_o, the mass flow rate m is given by [6]

$$\left(\frac{p}{p_o}\right)^{2/\gamma} - \left(\frac{p}{p_o}\right)^{(\gamma+1)/\gamma} = \left(\frac{\gamma - 1}{2\gamma}\right)\frac{m^2}{A^2 p_o \rho}$$

where p is the pressure (assumed uniform) at the point in the nozzle with cross section A and where discharge coefficient C_d has been introduced to express the efficiency of the nozzle.

This relation may be used to calculate the mass of gas leaving an aircraft through a window over a short time interval. The discharge leads to new upstream conditions which are then used to evaluate the flow for the next interval. A Fortran program was written to determine the upstream stagnation pressure as a function of time for parameter values representing the aircraft configuration, and this produced the time

history given in figure 13. This time history should be compared with the experimentally recorded time history shown in figure 11. The quasi-steady flow model is able to predict the overall drop in pressure within the aircraft cabin under decompression, but it is not able to predict the detailed staircase form of the initial part of the experimental result for which a non-steady flow model is required.

It is also interesting to consider the variation in temperature produced by the decompression. Under reversible adiabatic expansion it can be shown [6] that in an expansion from state 1 to state 2, the final temperature is related to the initial temperature

$$T_2 = T_1\left(\frac{p_2}{p_1}\right)^{(1-\gamma)/\gamma}$$

Assuming the ratio of specific heats, γ, of the gas is given by 1.4 and initial conditions of a gauge pressure of 1.3 bar and a temperature of 20°C (293.15K) the relation predicts a temperature drop of 21°C. This cooling is sufficient to cause some of the vaporised water in the compressed gas to condense into tiny droplets on expansion, and accounts for the fog observed in an aircraft undergoing a decompression which passengers often mistakenly believe to be smoke.

Non-Steady Flow

A discussion of non-steady flow often begins with a description of the effects of releasing a frictionless piston separating a region of high pressure from a region of low pressure in a tube of constant cross-section [7,8]. The difference in pressure on the two faces of the piston cause it to move towards the low pressure region. As it begins to move it produces a compression wavefront, or Mach wave, which travels at the speed of sound ahead of the piston and a rarefaction wavefront (Mach wave) behind it, also travelling at the speed of sound. As the piston continues to accelerate it produces infinitesimal Mach waves ahead and behind until the pressures on both sides are equal. The piston then moves at a constant velocity in the tube and no further Mach waves are produced. The state of the gas along the path of any of these Mach waves is constant but it changes infinitesimally across each wave. The decompression wave produced by the piston has a clearly defined beginning, at the time of piston release, and end, at the time when steady speed is attained. This concept may be applied to the substantially more difficult problem of three dimensional unsteady flow inside the aircraft.

As the gas close to the window starts to accelerate through the orifice a decompression wavefront is transmitted into the cabin. The rarefaction produces a local reduction in pressure. The gas continues to accelerate through the orifice producing further local

decompression until the local pressure falls by enough to produce steady flow through the orifice. At this point no further decompression waves are transmitted into the cabin. This idea is illustrated in figure 14.

The figure shows the progress of decompression waves on (x,t) axes. At t = 0, the orifice is opened and a decompression wavefront is transmitted into the cabin. The pressure at a transducer in the cabin a short distance from the window is steady until the arrival of the decompression wave front. As the compressed gas accelerates through the orifice further decompression Mach waves are produced and each of these is associated with a finite pressure reduction. The tail of the decompression wave is produced when the flow through the orifice becomes steady, and as this tail passes the transducer the pressure recorded is again steady.

The decompression wave propagates in the cabin until a solid surface is reached where the wave is reflected. The reflected wave then propagates back along the cabin towards the transducer which again records a pressure drop as the wave passes. On reaching the orifice further decompression waves are produced as the orifice flow velocity changes.

Each decompression Mach wave produces a local expansion of the compressed gas in the cabin, and consequently also a small temperature reduction. The speed of sound in a gas is proportional to the square root of the temperature and so this also reduces at each expansion. The whole compression wave therefore diverges as the tail of the wave propagates more slowly than the head of the wave.

Signal Interpretation

The two models discussed above give us an insight into the properties of the recorded pressure time history. The overall form of the time history is readily explained using the quasi-steady flow model, while the non-steady flow model qualitatively explains the staircase form of the initial part of the time history. The regions of completely steady pressure predicted by the non-steady flow model are not observed in practice because of reflections of the decompression wave from all surfaces within the cabin.

Interpretation of the accelerometer signal from a decompression is a little more difficult as there are two major components to excitation of the structure. The first component is caused by rupture of the diaphragm used to produce the decompression. The applied force is confined to a very small area (effectively the edge of the window) and is of short duration; it can be compared to a larger impulsive point load. The second applied force is due to the decompression wave which produces an excitation which is distributed over the entire surface of the cabin and which is of relatively long duration. The two

forms of excitation produce two distinct phases in the acceleration response signature. The response to the first component reaches a peak of 0.5g and is observed for a duration of 12ms. This is followed by the response to the local excitation produced by the arrival of the first decompression wave. The 12ms period is the time taken by the decompression wavefront to travel from the window to the sensor. The second phase of the acceleration time history reaches a peak of 4g and continues at a steady amplitude for about 0.4s while the pressure time history continues to show its staircase form. We note that the response levels of 0.5g and 4g for decompression are considerably smaller than the corresponding levels of 40g and 120g for blast.

The CVR signature also shows the diaphragm rupture response followed by the arrival of the first decompression wave (figure 5). The complete CVR signature (figure 3) also shows a low frequency amplitude variation. This pulsing of the response can be easily heard on playback of the CVR recording and can be seen more easily on a time-frequency spectrogram of the CVR signal. The pulse period is related to the time taken by the decompression wave to travel along the cabin length.

Conclusions

The simple models for blast and decompression have given an insight into the recorded accelerometer, pressure transducer and CVR signatures. Further refinements of the models could include a detailed investigation of wave reflection and refraction by cabin furnishings and a more detailed study of the aircraft vibration response. Several real air incidents have been considered by Slingerland [9,10] who has been able to identify the location in the aircraft of explosions and decompressions using a spectrogram method to analyse the vibration response of the CVR CAMs.

The experimental work has shown that there is a clear difference between the CVR signatures for blast and for decompression. Further work will consider the effects of a decompression produced by a blast wave rupturing a fuselage and other transient excitation phenomena. The aim is to give the accident investigators a set of CVR interpretation guidelines so that an early indication of the cause of failure of the aircraft can be obtained from the CVR recordings. This may be especially helpful when aircraft loss occurs over water since location of the source of a violent excitation will help to identify the wreckage parts which would be most likely to assist the accident investigators. Other types of transient event also need to be considered including CVR power bus switching, CAM energisation failure, and output open and short circuits - extremely violent events may separate the CVR recorder from the CAM which is usually installed in the tail of an aircraft.

Further experimental work may include measurements with CVRs from several manufacturers, including both analogue and digital types. Ideally measurements would be made on a wide variety of aircraft. The effects of background vibration and acoustic noise also need to be considered. This experimental work may lead to the development of an instrument dedicated to recording transient events on civil aircraft. Such an instrument could find applications in other surveillance operations including, for example, the record of an excitation history for fatigue monitoring and heavy-landing assessment.

Acknowledgement

This work has been carried out with the support of the Defence Research Agency (Fort Halstead). Their support is gratefully acknowledged. This paper was originally presented at Progrès Recents des Méthodes de Surveillance Acoustiques et Vibratoires, Senlis, France in October 1992 and permission from the Société Francaise des Mécaniciens to reproduce the paper is gratefully acknowledged.

References

[1] W E BRIERLEY and D J HAWKES (Chairmen), ED-56: Minimum operational performance requirements for cockpit voice recorder system, European organisation for civil aviation electronics, February 1988.

[2] S J C DYNE, The determination of the cause of failure of aircraft structures from transducer recordings up to the time of failure, ISVR CR 91/35, University of Southampton, December 1991.

[3] S J C DYNE, The determination of the cause of failure of aircraft structures from transducer recordings up to the time of failure, ISVR CR 92/17, University of Southampton, June 1992.

[4] A B MILLER, Research into the identification of the signatures of violent events in aircraft, Group working paper 2/92 (EC3), RARDE Fort Halstead, January 1992.

[5] G F KINNEY and K J GRAHAM, Explosive shocks in air, Springer-Verlag, 1985.

[6] B S MASSEY, Mechanics of fluids, Van Nostrand Reinhold, 1979.

[7] J A OWCZAREK, Fundamentals of gas dynamics, International Textbook Company, 1964.

[8] P A THOMPSON, Compressible fluid dynamics, McGraw Hill, 1972.

[9] F W SLINGERLAND, Spectrogram diagnosis of aircraft disasters, International Pacific Aerospace Conference, Gifu, Japan, October 1991.

[10] F W SLINGERLAND, Aircraft damage analysis by vibration spectrograms, National Research Council of Canada, Report LTR-ST-1572, February 1986.

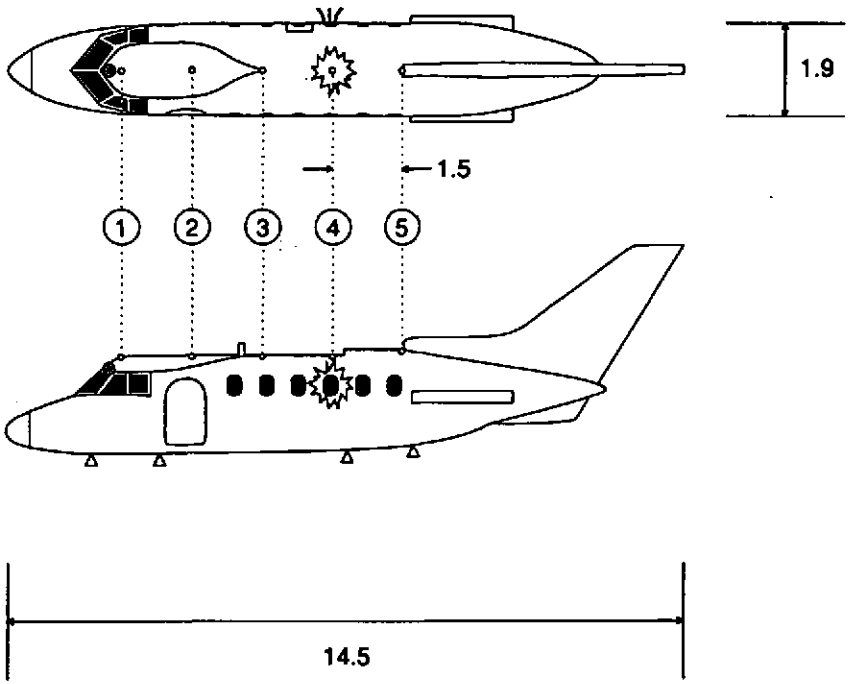

Figure 1: HS125 aircraft showing the location of the pressure transducers, the diaphragm and the explosive charges. The output from pressure transducer 4 is shown in figures 10 and 11 below.

CVR RECORDERS

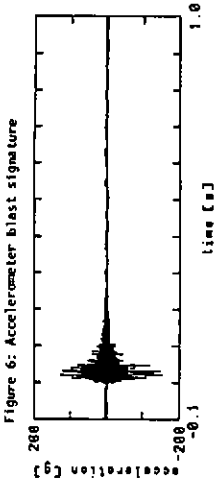

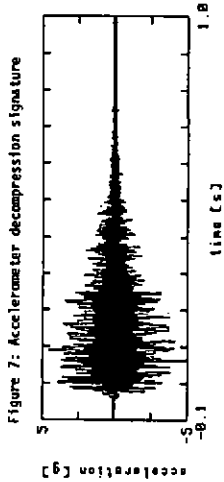

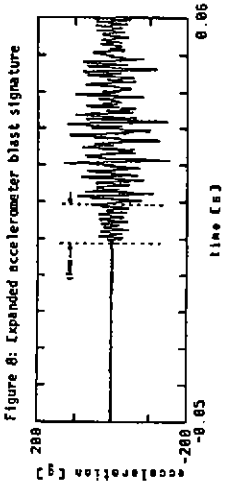

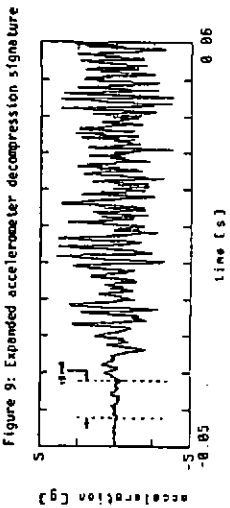

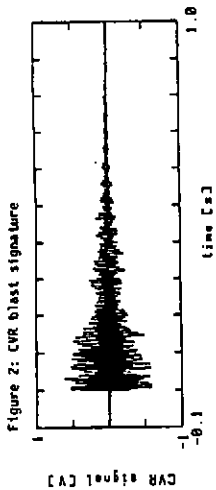

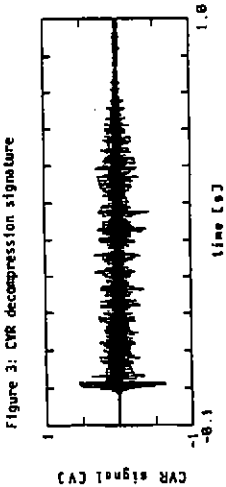

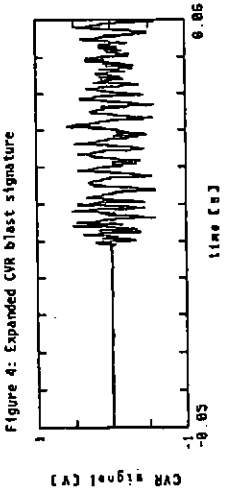

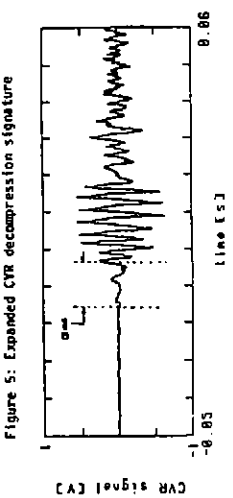

Figure 10: Pressure transducer 4 output for blast

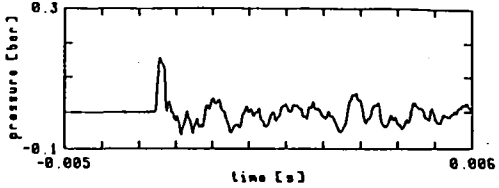

Figure 11: Pressure transducer 4 output for decompression

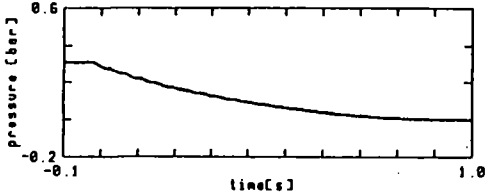

Figure 12: Idealised form of blast wave

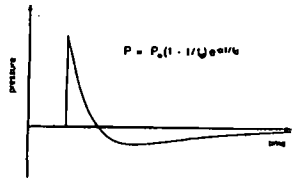

Figure 13: Quasi steady-flow model pressure prediction

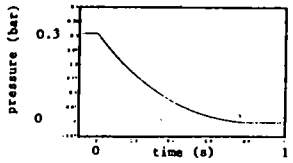

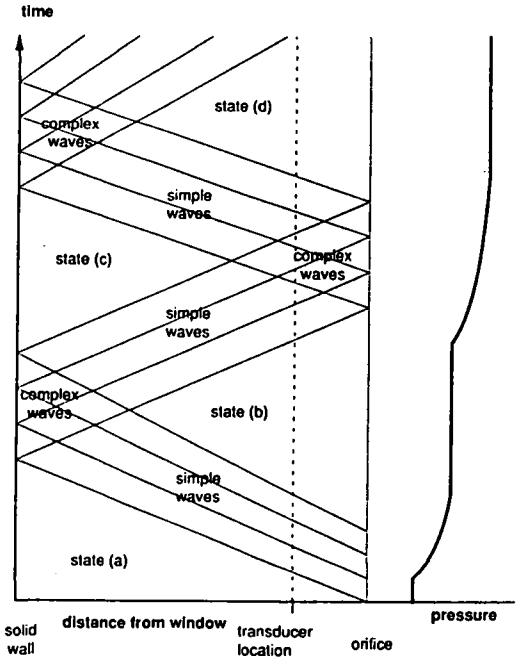

Figure 14: Distance-time plot showing the progress of the rarefaction waves into the aircraft fuselage following diaphragm rupture. The plot also shows the resulting time history of a pressure transducer in the flow.